






The effect of osteocyte-derived RANKL on bone graft remodeling: An in vivo experimental study

Balazs Feher^{1,2,3}  | Carina Kamplleitner^{4,5,6} | Patrick Heimel^{4,5,6} | Stefan Tangl^{4,5}  |
Jill A. Helms⁷  | Ulrike Kuchler²  | Reinhard Gruber^{1,5,8} 

¹Department of Oral Biology, University Clinic of Dentistry, Medical University of Vienna, Vienna, Austria

²Department of Oral Surgery, University Clinic of Dentistry, Medical University of Vienna, Vienna, Austria

³Department of Oral Medicine, Infection, and Immunity, Harvard School of Dental Medicine, Boston, Massachusetts, USA

⁴Karl Donath Laboratory for Hard Tissue and Biomaterial Research, University Clinic of Dentistry, Medical University of Vienna, Vienna, Austria

⁵Austrian Cluster for Tissue Regeneration, Vienna, Austria

⁶Ludwig Boltzmann Institute for Traumatology, The Research Center in Cooperation with AUVA, Vienna, Austria

⁷Department of Surgery, School of Medicine, Stanford University, Palo Alto, California, USA

⁸Department of Periodontology, School of Dental Medicine, University of Bern, Bern, Switzerland

Correspondence

Reinhard Gruber, Department of Oral Biology, University Clinic of Dentistry, Medical University of Vienna, Vienna, Austria.

Email: reinhard.gruber@meduniwien.ac.at

Funding information

International Team for Implantology; Osteology Foundation

Abstract

Objectives: Autologous bone is considered the gold standard for grafting, yet it suffers from a tendency to undergo resorption over time. While the exact mechanisms of this resorption remain elusive, osteocytes have been shown to play an important role in stimulating osteoclastic activity through their expression of receptor activator of NF- κ B (RANK) ligand (RANKL). The aim of this study was to assess the function of osteocyte-derived RANKL in bone graft remodeling.

Materials and Methods: In *Tnfsf11^{fl/fl};Dmp1-Cre* mice without osteocyte-specific RANKL as well as in *Dmp1-Cre* control mice, 2.6 mm calvarial bone disks were harvested and transplanted into mice with matching genetic backgrounds either subcutaneously or subperiosteally, creating 4 groups in total. Histology and micro-computed tomography of the grafts and the donor regions were performed 28 days after grafting.

Results: Histology revealed marked resorption of subcutaneous control *Dmp1-Cre* grafts and new bone formation around subperiosteal *Dmp1-Cre* grafts. In contrast, *Tnfsf11^{fl/fl};Dmp1-Cre* grafts showed effectively neither signs of bone resorption nor formation. Quantitative micro-computed tomography revealed a significant difference in residual graft area between subcutaneous and subperiosteal *Dmp1-Cre* grafts ($p < .01$). This difference was not observed between subcutaneous and subperiosteal *Tnfsf11^{fl/fl};Dmp1-Cre* grafts ($p = .17$). Residual graft volume ($p = .08$) and thickness ($p = .13$) did not differ significantly among the groups. Donor area regeneration was comparable between *Tnfsf11^{fl/fl};Dmp1-Cre* and *Dmp1-Cre* mice and restricted to the defect margins.

Conclusions: The results suggest an active function of osteocyte-derived RANKL in bone graft remodeling.

KEYWORDS

biomedical, bone regeneration, bone transplantation, mice, oral, surgery, transgenic, translational research

This is an open access article under the terms of the [Creative Commons Attribution-NonCommercial](https://creativecommons.org/licenses/by-nc/4.0/) License, which permits use, distribution and reproduction in any medium, provided the original work is properly cited and is not used for commercial purposes.

© 2023 The Authors. *Clinical Oral Implants Research* published by John Wiley & Sons Ltd.

1 | INTRODUCTION

Bone grafting leverages the intrinsic regenerative capacity of the bone to correct alveolar bone deficiencies and enable optimal implant placement (Dimitriou et al., 2011; Salem et al., 2016). Autologous (i.e., harvested from the same individual) bone is generally considered the gold standard for grafting as it contains viable osteogenic cells, intrinsic growth factors, and a scaffold that collectively promotes new bone formation (Chen et al., 2023; Hjørting-Hansen, 2002; Troeltzsch et al., 2016). As part of the integration process, bone grafts are subject to internal resorption. This resorption is coupled with new bone formation to achieve a union between the host bone and the graft (Bauer & Muschler, 2000; Stevenson et al., 1991). However, autologous bone grafts placed as onlays, outside the confines of the skeleton, are also subject to surface resorption over time (Lee et al., 2022; Stricker et al., 2021). In contrast to internal graft resorption, which is necessary to initiate graft integration, surface resorption leads to a reduction in graft volume. Over 40% of an autologous bone graft is resorbed in the first 12 postoperative months (Stricker et al., 2021); near-complete resorption can be observed after 6 years (Sbordone et al., 2012). This is a considerable limiting factor for the long-term stability at the site of bone grafting and, by extension, the success of dental implants placed in regenerated bone. Clinically, one suggestion to reduce surface resorption has been to combine or substitute autologous bone with allogeneic [i.e., harvested from a different individual of the same species (Meza-Mauricio et al., 2022)], xenogeneic [i.e., harvested from a different species (Maiorana et al., 2005)], or synthetic [e.g., β -tricalcium phosphate (Mendes et al., 2022)] material. Notwithstanding this clinical practice, the question of why autologous grafts resorb is yet to be answered. Much remains elusive with regard to the underlying cellular mechanisms that trigger graft resorption. On a basic level, graft resorption itself could plausibly be compared to bone resorption during physiological remodeling.

During bone remodeling, osteoclasts resorb old or damaged bone (Hattner et al., 1965). Receptor activator of NF- κ B (RANK) ligand (RANKL) is a key factor for the differentiation and activity of osteoclasts (Insogna et al., 1997; Kong et al., 1999). A member of the tumor necrosis factor family, RANKL is encoded by the *Tnfsf11* gene and primarily expressed by osteocytes (Nakashima et al., 2011; Xiong et al., 2011). Osteoblasts and lining cells also express RANKL (Ono et al., 2020; Xiong & O'Brien, 2012), yet osteoclast formation in bone remodeling is mainly driven by osteocyte-derived RANKL (Xiong et al., 2015). By binding to RANK on osteoclast precursors, RANKL triggers their differentiation into mature osteoclasts and thus allows for bone resorption (Park et al., 2017). During physiological bone remodeling, resorption is coupled with bone formation (Andersen et al., 2013; Delaisse, 2014). It is apparent that as the primary source of RANKL, osteocytes exert significant control over osteoclasts and the process of resorption during remodeling (Nakashima et al., 2011; Xiong et al., 2011; Xiong et al., 2015). In addition to physiological bone remodeling, recent evidence has shed light on the role of RANKL expression in osteocytes in both iatrogenic settings

[e.g., orthodontic tooth movement (Shoji-Matsunaga et al., 2017)] and pathological circumstances [e.g., calcium or estrogen deficiency, periodontal bone loss (Fujiwara et al., 2016; Graves et al., 2018; Xiong et al., 2014)]. It is therefore reasonable to assume that RANKL expression in osteocytes plays a role in bone graft remodeling as well.

Most of our present knowledge about the role of osteocytic signaling, including the role of RANKL expression in osteocytes, is derived from murine Cre/loxP conditional knockout systems (Kim et al., 2018) utilizing dentin matrix phosphoprotein 1 (*Dmp1*) (Chicana et al., 2022; Ding et al., 2022; Fujiwara et al., 2016; Graves et al., 2018; Lim et al., 2021; Nakashima et al., 2011; Shoji-Matsunaga et al., 2017; Xiong et al., 2011; Xiong et al., 2014; Xiong et al., 2015). *Dmp1* is an extracellular matrix protein that is present in dental and bone tissue where it is primarily expressed by odontoblasts as well as mature osteoblasts and osteocytes, respectively (Fen et al., 2002; George et al., 1993; Komori, 2014; Toyosawa et al., 2001). In this study, we used a Cre/loxP conditional knockout system to selectively silence the RANKL-encoding *Tnfsf11* gene in *Dmp1*-expressing cells. We hypothesized that silencing osteocyte-derived RANKL leads to suppression of the graft resorption; we further hypothesized this suppression of resorption ultimately prevents new bone formation. To test these hypotheses, we bred mice lacking RANKL expression in osteocytes. We then harvested bone disks from the calvariae of mice lacking osteocyte-derived RANKL and transplanted them as grafts. To control for a potential effect of the host bone, we transplanted the grafts into both subcutaneous (i.e., no contact to host bone) and subperiosteal (i.e., direct contact to host bone) environments. As controls to our experimental models, we used mice with uninhibited osteocyte-derived RANKL expression in osteocytes.

2 | MATERIALS AND METHODS

All experimental protocols were approved by the Medical University of Vienna institutional animal care and use committee as well as the Austrian Federal Ministry of Education, Science, and Research (No. 2020-0.225.666). Reporting followed ARRIVE guidelines (Kilkenny et al., 2010).

2.1 | Experimental animals

B6N.FVB-Tg(*Dmp1-cre*)1Jqfe/BwdJ (*Dmp1-Cre* mice, strain 023047) and B6.129-Tnfsf11^{tm1.1Caob/J} (*Tnfsf11*^{fl/+} mice, strain 018978) were commercially obtained (Jackson Laboratory, Bar Harbor, ME, USA) and subsequently crossed (Core Facility Laboratory Animal Breeding and Husbandry, Medical University of Vienna, Himberg, Austria) to generate lineage-specific *Tnfsf11*^{fl/fl}; *Dmp1-Cre* mice. Through this action, the RANKL-encoding *Tnfsf11* gene was knocked out in *Dmp1*-expressing cells and mature osteoblasts and osteocytes of these mice were rendered unable to express RANKL. This process was controlled by routine genotyping of all animals (Transnetyx, Munich,

Germany). *Tnfsf11^{fl/fl};Dmp1-Cre* mice further exhibit an evident osteopetrotic phenotype which was observed using micro-computed tomography (Figure S1). Care and attention were paid to good animal care and treatment. Animals were kept in species-appropriate cages, in groups of 5 or fewer mice of the same genotype each. A 1:1 day/night rhythm was set, and all animals received water and a regular diet ad libitum. An acclimatization period of at least 7 days was provided to all animals preoperatively. The temperature in the rooms where the animals were kept was set to $22 \pm 2^\circ\text{C}$ and the relative humidity was $55 \pm 10\%$. All animals were routinely weighed before and after surgery. Surgeries were performed on 8-week-old mice of both sexes which weighed $21 \pm 3\text{g}$ preoperatively. Postoperative monitoring was performed by veterinarians (Center for Biomedical Research and Translational Surgery, Medical University of Vienna, Vienna, Austria) and by the operating surgeons. The exclusion of an animal from the study was strictly regulated based on humane endpoints: drastic weight loss, reduced physical condition, obvious pain, as well as behavioral problems would lead to the exclusion of an animal from the study.

2.2 | Surgical protocol

In 8-week-old *Tnfsf11^{fl/fl};Dmp1-Cre* and *Dmp1-Cre* mice, general anesthesia was induced by first placing the animals in a closed container permeated with a mixture of isoflurane and oxygen vapor at 4% volume concentration for 2 min, then injecting a combination of medetomidine 0.3mg kg^{-1} , midazolam 1mg kg^{-1} , fentanyl 0.03mg kg^{-1} , and ketamine 10mg kg^{-1} subcutaneously. The back of the head was shaved using an electric razor and the surgical site was disinfected with povidone-iodine. Using a No. 15 surgical blade, a 6 mm long parasagittal incision was made 1 mm left of the sagittal suture. After preparing a full-thickness flap, a trephine drill with an inner diameter of 2.6 mm and an outer diameter of 3.2 mm was used to remove a bone disk from the left parietal bone. The trephine drill was used in as counterclockwise direction to minimize tissue damage, and manual irrigation using a 0.9% saline solution was used. As autologous transplantation in rodents is unnecessarily stressful, the bone disk was transplanted into a different mouse of the same genetic background to simulate autologous grafting based on previous literature (Huang et al., 2022; Leucht et al., 2013). For subcutaneous placement, a 3 mm long parasagittal superficial incision was made 1 mm right of the sagittal suture, and the bone disk was placed under the subcutaneous pouch. For subperiosteal placement, no additional incision was made, and the periosteum was elevated from the right parietal bone where the bone disk was then placed. In both cases, the extracorporeal time of the graft did not exceed 2 min. Wounds were closed with interrupted resorbable monofilament USP 6-0 sutures. Anesthesia was antagonized by injecting a combination of atipamezole 1mg kg^{-1} and flumazenil 0.1mg kg^{-1} subcutaneously. To control postoperative pain, a single dose of buprenorphine 0.06mg kg^{-1} was administered by subcutaneous injection after regaining consciousness, followed by piritramide 0.068mg mL^{-1} orally with drinking

water for 72 h. Mice were euthanized after a total of 28 days in line with previous research (Chen et al., 2020; Zhang et al., 2005).

2.3 | Histology

For the histological analysis, tissues were first fixed in 4% formalin, then dehydrated in ascending grades of ethanol, and finally embedded in light-cured resin (Technovit 7200 VLC + 1% benzoyl peroxide, Kulzer, Hanau, Germany). Resin blocks were further processed using cutting and grinding equipment (Exakt Apparatebau, Norderstedt, Germany). Undecalcified thin-ground sections were prepared parallel to the sagittal suture and through the center of the bone graft or defect and were stained with Levai-Laczko dye for descriptive histology. In this staining, woven bone appears dark pink, mature lamellar bone light pink, and soft tissue blue. The osteoid remains unstained. Digital pictures were obtained with a digital virtual microscopy system (dotSlide 2.4, Olympus, Shinjuku, Japan) at a resolution of $0.32\ \mu\text{m px}^{-1}$.

2.4 | Micro-computed tomography

Ex vivo micro-computed tomography scans were performed at 90 kV and $200\ \mu\text{A}$ with an isotropic resolution of $20.7\ \mu\text{m}$ ($\mu\text{CT 50}$, SCANCO Medical AG, Bruttisellen, Switzerland). Scans were three-dimensionally reconstructed using a visualization software (Amira 6.1.1., Thermo Fisher Scientific, Waltham, MA, USA). To analyze the bone graft and donor area, image stacks were rotated, so that the bone disk or the donor area was aligned to the XY-plane.

For the graft, the region of interest (ROI) was defined as the right circular cylinder aligned to the graft center with a base ($d = 2.5\text{ mm}$) parallel to the graft surface area and an individually set height for each scan to yield the smallest possible volume still containing the entire graft. Around the circular osteotomy area where the graft was harvested ($d = 3.2\text{ mm}$), a cylindrical shell-shaped ROI (zone of death, $d_d = 250\ \mu\text{m}$) was defined in accordance with current literature on the effect of trauma at osteotomy sites on osteocytes (Wang et al., 2017). In addition, a second cylindrical shell-shaped ROI with the same width (safety zone, $d_s = 250\ \mu\text{m}$) was defined around the zone of death. The heights of the cylindrical shells were also set individually to yield the smallest possible volume still containing the calvaria in its entire thickness. All measurements were performed using an open-source image processing program (ImageJ, National Institutes of Health, Bethesda, MD, USA) with a custom-defined ruleset.

2.5 | Statistical analysis

Data are presented as means and standard deviations unless stated otherwise. Our preliminary sample size calculation was reviewed by the Medical University of Vienna institutional animal care and

use committee prior to approval. The primary parameters of this study were residual graft area (i.e., the surface area of the graft after 28 days as a fraction of the surface area of original graft), residual graft volume (i.e., the volume of the graft after 28 days as a fraction of the volume of the original graft), and graft thickness (i.e., the average thickness of the graft after 28 days), as measured with micro-computed tomography. The secondary parameter of this study was bone volume fraction (bone volume per total volume, BV/TV) in the donor area, as measured with micro-computed tomography. The sample size was calculated a priori based on the relative residual graft area: we set a clinically relevant threshold of a 30% smaller remaining area in at least one of the four groups. This resulted in a minimal sample size of 4 plus dropouts per group (16 animals plus dropouts for the whole study). For this study, a total of 21 animals were used, with the following allocation: 6 mice in the subperiosteal Dmp1-Cre graft group, 6 mice in the subcutaneous Dmp1-Cre graft group, 5 mice in the subperiosteal *Tnfsf11^{fl/fl};Dmp1-Cre* graft group, and 4 mice in the subcutaneous *Tnfsf11^{fl/fl};Dmp1-Cre* graft group. The final number of animals was a function of the availability of animals of different genotypes. The ordinary one-way analysis of variance (ANOVA) and Holm-Sidak post-hoc tests were used to compare primary parameters between groups. Unpaired Student's t-tests were used to compare the secondary parameters between groups. Histological analysis is presented in a descriptive manner. Where hypothesis testing was performed, a *p*-value <.05 was considered significant. Statistical analysis was performed using Prism 9.5.1 (GraphPad Software, Boston, MA, USA).

3 | RESULTS

3.1 | Grafts lacking osteocyte-derived RANKL display no histological signs of bone resorption or formation

To study the effect of osteocyte-derived RANKL on bone graft remodeling, grafts harvested from the left parietal bone of *Tnfsf11^{fl/fl};Dmp1-Cre* mice with silenced osteocytic RANKL expression as well as from Dmp1-Cre control mice were transplanted into subcutaneous pouches and as subperiosteal onlays. One animal in the subperiosteal *Tnfsf11^{fl/fl};Dmp1-Cre* graft group was lost due to intraoperative complications. The postoperative phase was uneventful, with no complications and no further loss of animals. A total of 20 animals were included in all analyses. Histological analysis showed neglectable signs of bone resorption or formation around *Tnfsf11^{fl/fl};Dmp1-Cre* grafts. While subcutaneous Dmp1-Cre grafts showed prominent resorption (Figure 1a,c), the edges of subcutaneous *Tnfsf11^{fl/fl};Dmp1-Cre* grafts remained continuous and uninterrupted (Figure 1b,e). We further found a more marked presence of multinucleated osteoclast-like cells in close proximity to the subcutaneous Dmp1-Cre grafts (Figure 1d) compared with subcutaneous *Tnfsf11^{fl/fl};Dmp1-Cre* grafts (Figure 1f). When placed subperiosteally, Dmp1-Cre grafts showed new bone formation on both the graft and the host side (Figure 2a,d). In contrast, subperiosteal *Tnfsf11^{fl/fl};Dmp1-Cre* grafts showed minimal amounts of new woven bone (Figure 2b,f). Notably, the side of the subperiosteal Dmp1-Cre graft facing away from the host showed some resorption (Figure 2c).

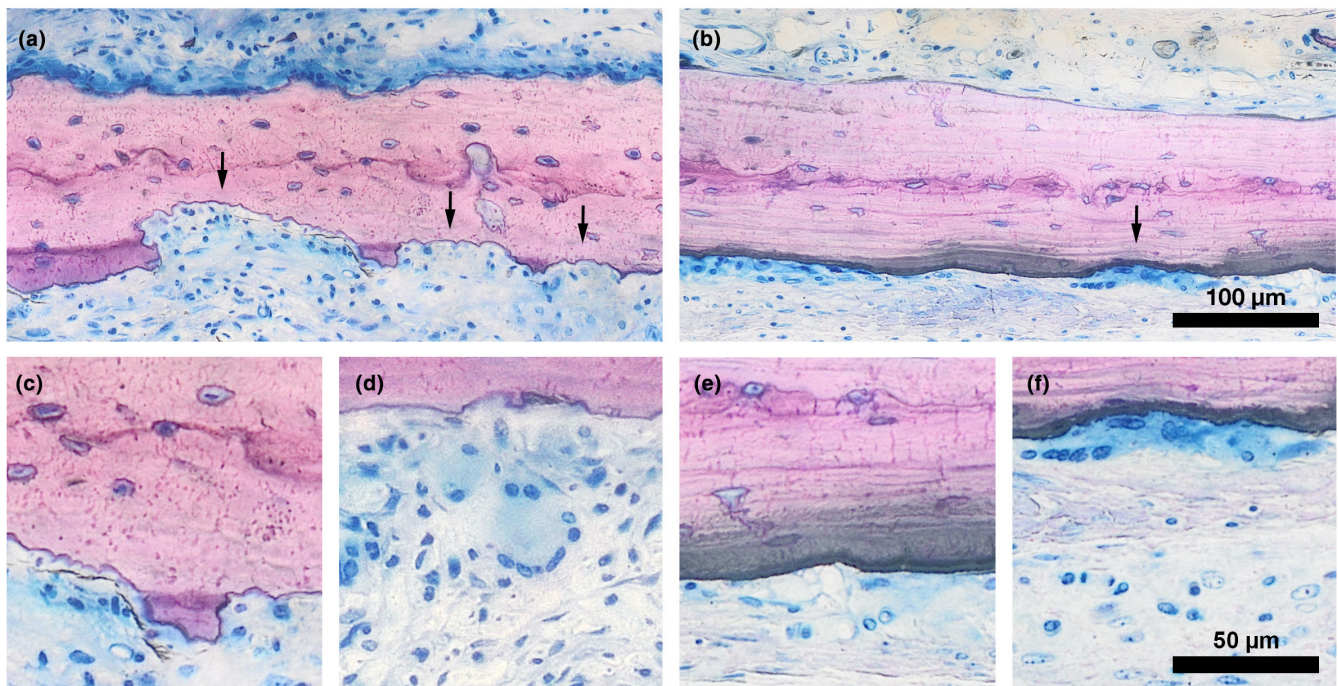


FIGURE 1 Histological overview of subcutaneous grafts. (a, c, d) Dmp1-Cre graft (*n*=6). (b, e, f) *Tnfsf11^{fl/fl};Dmp1-Cre* graft (*n*=4); Black arrows denote preceding resorption areas.

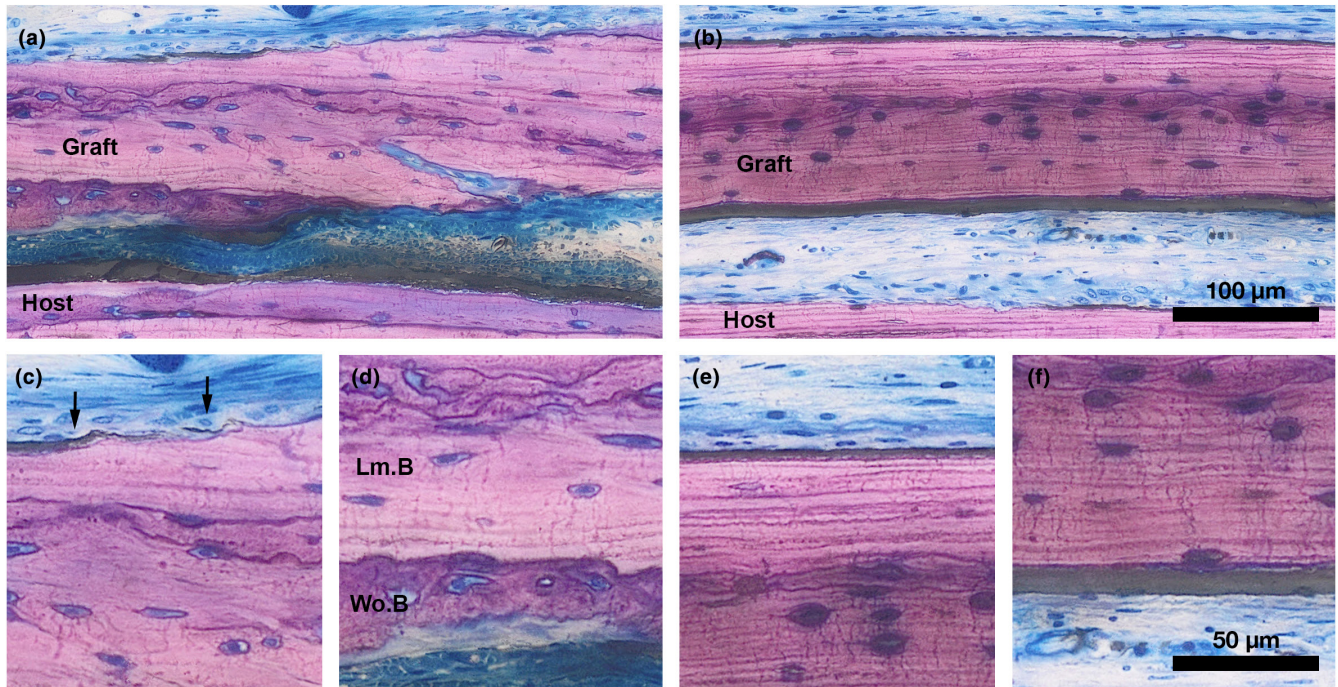


FIGURE 2 Histological overview of subperiosteal grafts. (a, c, d) Dmp1-Cre graft ($n=6$). (b, e, f) Tnfsf11^{fl/fl};Dmp1-Cre graft ($n=4$). Black arrows denote irregular surface of Dmp1-Cre grafts compared to Tnfsf11^{fl/fl};Dmp1-Cre grafts. Lm.B, lamellar bone; Wo.B, woven bone.

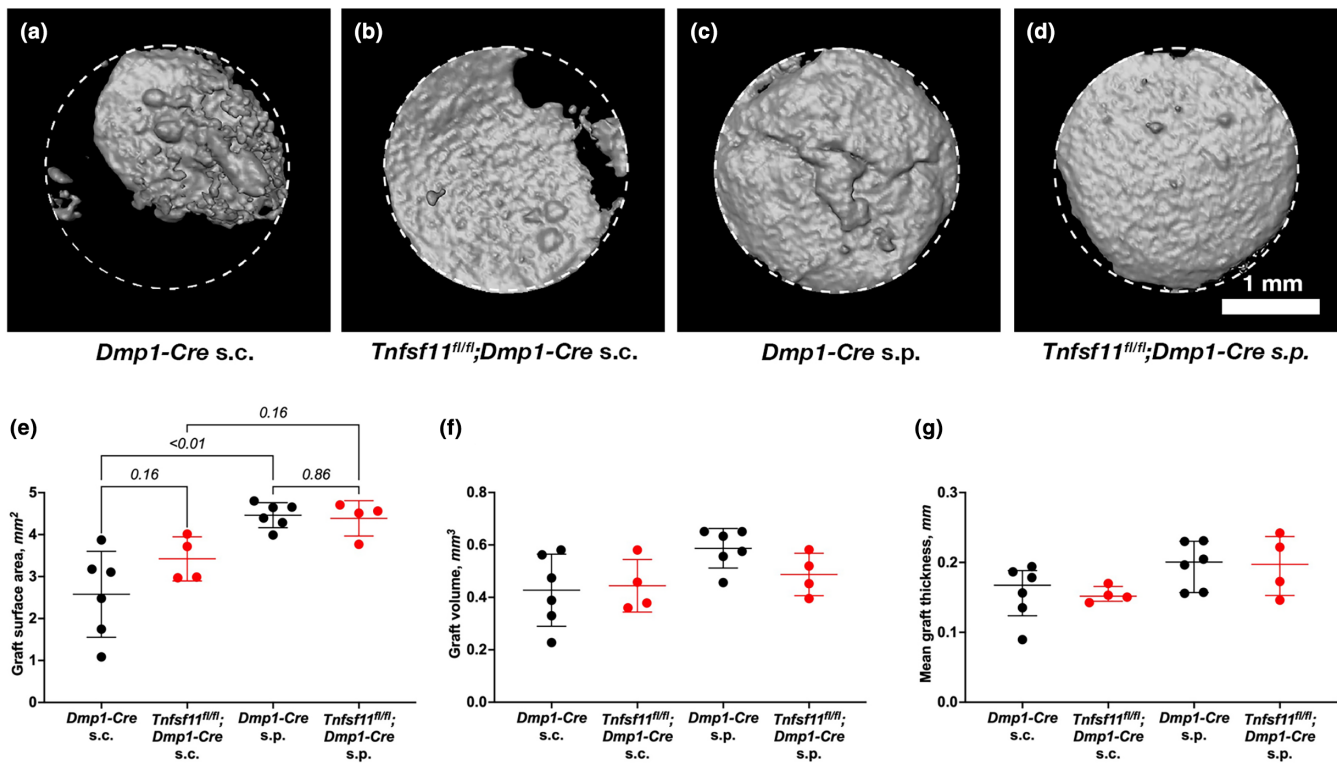


FIGURE 3 Ex vivo micro-computed tomography of the grafts after 4 weeks. (a–d) Overview of the grafts. (e) Residual graft surface area ($p < .01$). (f) Residual graft volume ($p = .08$). (g) Mean residual graft thickness ($p = .13$). Bars and error bars show means and standard deviations, p -values in figure legend using one-way ANOVA, p -values in graph using Holm-Sidak post hoc tests. All results include data from both male and female mice. S.c., subcutaneous; s.p., subperiosteal.

This, too, could not be observed in subperiosteal *Tnfsf11^{fl/fl};Dmp1-Cre* grafts whose outer surface remained uninterrupted (Figure 2e). Taken together, the histological results suggest that silencing osteocyte-derived RANKL prevents bone grafts from undergoing both resorption and new bone formation.

3.2 | Silencing osteocyte-derived RANKL reduces radiographic resorption of ectopic grafts

Remodeling over the 28-day healing period was quantified using micro-computed tomography of the grafts (Figure 3). Subcutaneous *Dmp1-Cre* grafts showed the lowest residual area at $2.6 \pm 1.0 \text{ mm}^2$, compared to subcutaneous *Tnfsf11^{fl/fl};Dmp1-Cre* grafts at $3.4 \pm 0.5 \text{ mm}^2$, subperiosteal *Tnfsf11^{fl/fl};Dmp1-Cre* grafts at $4.4 \pm 0.4 \text{ mm}^2$, and subperiosteal *Dmp1-Cre* grafts at $4.5 \pm 0.3 \text{ mm}^2$. The difference among these four groups was significant ($p < .01$). Post-hoc tests revealed a significant difference between subcutaneous and subperiosteal *Dmp1-Cre* grafts ($p < .01$), but no significant differences between subcutaneous *Dmp1-Cre* and *Tnfsf11^{fl/fl};Dmp1-Cre* grafts ($p = .16$), subperiosteal *Dmp1-Cre* and *Tnfsf11^{fl/fl};Dmp1-Cre* grafts ($p = .86$), as well as subcutaneous and subperiosteal *Tnfsf11^{fl/fl};Dmp1-Cre* grafts ($p = .16$) (Figure 3e).

Subcutaneous *Dmp1-Cre* grafts also showed the lowest graft volume at $0.43 \pm 0.14 \text{ mm}^3$, compared to subcutaneous *Tnfsf11^{fl/fl};Dmp1-Cre* grafts at $0.44 \pm 0.10 \text{ mm}^3$, subperiosteal *Tnfsf11^{fl/fl};Dmp1-Cre* grafts at $0.49 \pm 0.08 \text{ mm}^3$, and subperiosteal *Dmp1-Cre* grafts at $0.59 \pm 0.08 \text{ mm}^3$. The difference among these four groups was not significant ($p = .08$) (Figure 3f). Subcutaneous *Tnfsf11^{fl/fl};Dmp1-Cre* grafts showed the lowest mean graft thickness at $0.15 \pm 0.01 \text{ mm}$, compared to subcutaneous *Dmp1-Cre* grafts at $0.16 \pm 0.04 \text{ mm}$, subperiosteal *Dmp1-Cre* grafts at $0.20 \pm 0.03 \text{ mm}$, and subperiosteal *Tnfsf11^{fl/fl};Dmp1-Cre* grafts at $0.20 \pm 0.04 \text{ mm}$. The difference among these four groups was not significant ($p = .13$) (Figure 3g). Taken together, the results of the quantitative micro-computed tomography suggest that osteocyte-derived RANKL triggers negative changes in the graft surface area. Subperiosteal placement seems to counteract this catabolic effect.

3.3 | Calvarial donor sites do not regenerate irrespective of osteocyte-derived RANKL

The potential effect of osteocyte-derived RANKL on the donor site, a critical-sized calvarial defect in itself, was analyzed using both histology and micro-computed tomography of the parietal bone. After 28 days of healing, both *Tnfsf11^{fl/fl};Dmp1-Cre* and *Dmp1-Cre* donor

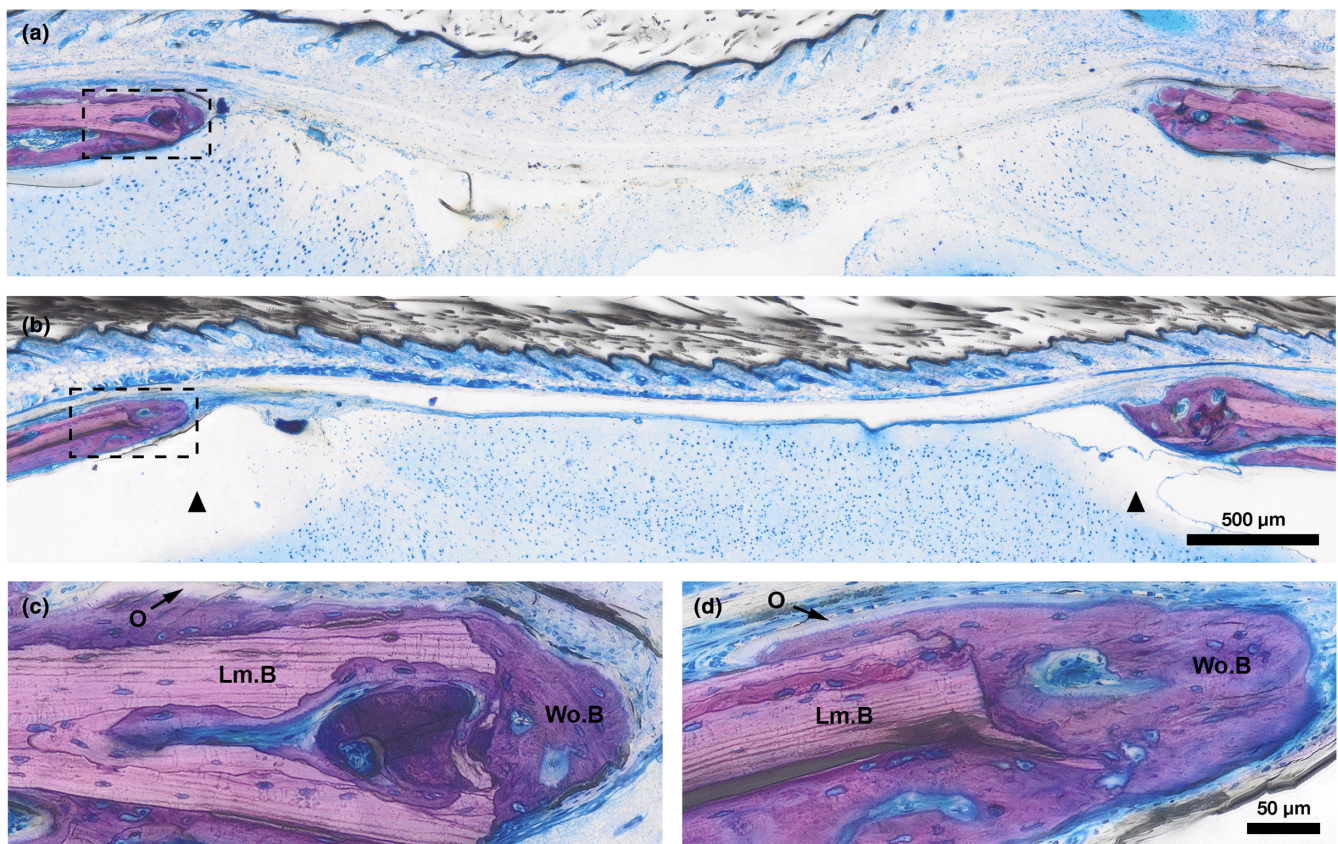


FIGURE 4 Histological overview of the donor area. (a, c) *Dmp1-Cre* mouse. (b, d) *Tnfsf11^{fl/fl};Dmp1-Cre* mouse. Black triangles indicate the defect edges. Lm.B, lamellar bone (light pink); O, osteoid (unstained); Wo.B, woven bone (dark pink).

sites showed little bone regeneration which was largely restricted to the defect margins (Figure 4a,b). While the edges of the osteotomy were surrounded by new woven bone (Figure 4c,d), defect coverage remained minimal. For quantitative micro-computed tomography, the circular osteotomy area, the zone of death, and the safety zone were set as ROIs (Figure 4b,d-f). No significant difference in BV/TV could be observed between *Tnfsf11^{fl/fl};Dmp1-Cre* and *Dmp1-Cre* mice in either the zone of death ($p = .72$) or the safety zone ($p = .13$) (Figure 4g,h). Taken together, the results suggest that osteocyte-derived RANKL has no effect on the regeneration of calvarial donor sites which itself, however, is limited to the defect margins.

4 | DISCUSSION

Since the implementation of autologous onlay bone grafts in clinical dentistry, long-term outcomes have been limited by their surface resorption (Stricker et al., 2021), leading to the clinical practice of using combined grafts and stimulating a debate about whether pure autografts can be considered the gold standard (Sakkas et al., 2017; Zhao et al., 2021). While in bone biology, the mechanisms of osteoclastogenesis, in general, have largely been deciphered—including the crucial role of osteocytes through their RANKL expression—the causes of autograft resorption have remained unclear. Our findings now shed some light on these processes, as we have made the important discovery that silencing RANKL in osteocytes has a major impact on the resorption of the graft. Grafts harvested from and transplanted into mice without osteocyte-derived RANKL remained virtually unreactive, showing neglectable signs of either resorption or new bone formation. This was in stark contrast to grafts harvested from and transplanted into mice without with undisturbed osteocytic expression of RANKL. The latter showed substantial resorption when placed subcutaneously, and resorption as well as visible new bone formation when placed subperiosteally.

The present study is the first to use a lineage-specific conditional knockout model to study the role of osteocyte-derived RANKL in bone graft remodeling. As our model involved transplantation between matching genotypes, we are not able to draw conclusions with regard to the role of osteocyte-derived RANKL in the graft versus the host. Nevertheless, our data support previous findings with regard to the link between osteocyte-derived RANKL per se and bone resorption in both health and disease. Previous research using conditional knockout murine models has identified osteocyte-derived RANKL to be a primary regulator of bone homeostasis by driving resorption during physiological remodeling (Nakashima et al., 2011; Xiong et al., 2011). In addition, osteocyte-derived RANKL also mediates inflammatory osteolysis, as shown in a lipopolysaccharide-induced murine periodontitis model (Graves et al., 2018). Our findings add to this knowledge and extend it toward the resorption of bone grafts. Histologically, osteocytes inside the bone harvested from murine calvaria appear to be viable following transplantation (Figures 1 and 2), lending credence to the hypothesis that their

RANKL expression has an effect on graft remodeling. At first sight, our observations could be linked to bone regeneration rather than bone remodeling. However, our data from subperiosteal grafts show that new bone formation also seems to be impaired by the lack of RANKL in osteocytes, supporting the general principle that resorption and formation are coupled.

The clinical relevance of our observations remains at a speculative level. Our findings are consistent with the clinical observation that adequately placed bone grafts do not provoke an immediate, excessive immune response and thus only show moderate resorption in the initial postoperative period. However, our short follow-up time of 28 days must be taken into consideration. The clinical practice of limiting effective resorption by combining autologous bone with different graft materials stems from the obvious necessity of long-term graft retention. Previous clinical research on pure autologous grafts has shown a mean resorption of 44% after 12 months (Stricker et al., 2021) and near-complete resorption after 6 years (Sbordone et al., 2012). In contrast, our previous long-term case series on combined autologous-xenogeneic grafts has shown a mean resorption of 25% after a median of 7 years (Feher et al., 2022). Notwithstanding our considerably shorter follow-up period in the current preclinical study, our data still suggest the bony environment protects subperiosteal grafts—even with intact osteocytic expression of RANKL—as subperiosteal grafts displayed minimal to no resorption. In contrast, placing the grafts away from the host bone and periosteum obviously initiated a catabolic environment, which drove osteoclastogenesis and in turn, graft resorption.

This observation raises the obvious question of why we see such marked resorption in subcutaneous *Dmp1-Cre* grafts when compared with subperiosteal grafts. One possible reason is inflammatory osteolysis, a clinically unwanted phenomenon which in this case has luckily allowed us to discover that osteocyte-derived RANKL is required for graft resorption. At the molecular level, the question remains what exactly triggers osteocytes within the graft to express RANKL. Importantly, histology has revealed viable osteocytes inside the graft. Therefore, one possible explanation is that osteocytic apoptosis at the graft margins triggers RANKL expression in the remaining viable bystander osteocytes (McCutcheon et al., 2020). An entirely different explanation is that following apoptosis, the secondary osteocytic necrosis results in the direct stimulation of osteoclasts via damage-associated molecular patterns (DAMPs) (Andreev et al., 2020). Notwithstanding previous data from a murine model supporting this DAMP-dependent mechanism of osteoclastogenesis, our data underscore the role of osteocyte-derived RANKL, for at ostensibly consistent levels of osteocytic apoptosis—and by extension, secondary necrosis—between the study groups, they have shown markedly different patterns of resorption.

As the role of inflammation in triggering osteolysis has previously been demonstrated (Graves et al., 2018), another open question of potential clinical relevance is whether intervening in the inflammatory cascade (e.g., by an anti-inflammatory agent) would lead to different outcomes. Traditional non-steroidal anti-inflammatory drugs typically target both cyclooxygenase (COX) 1 and COX-2

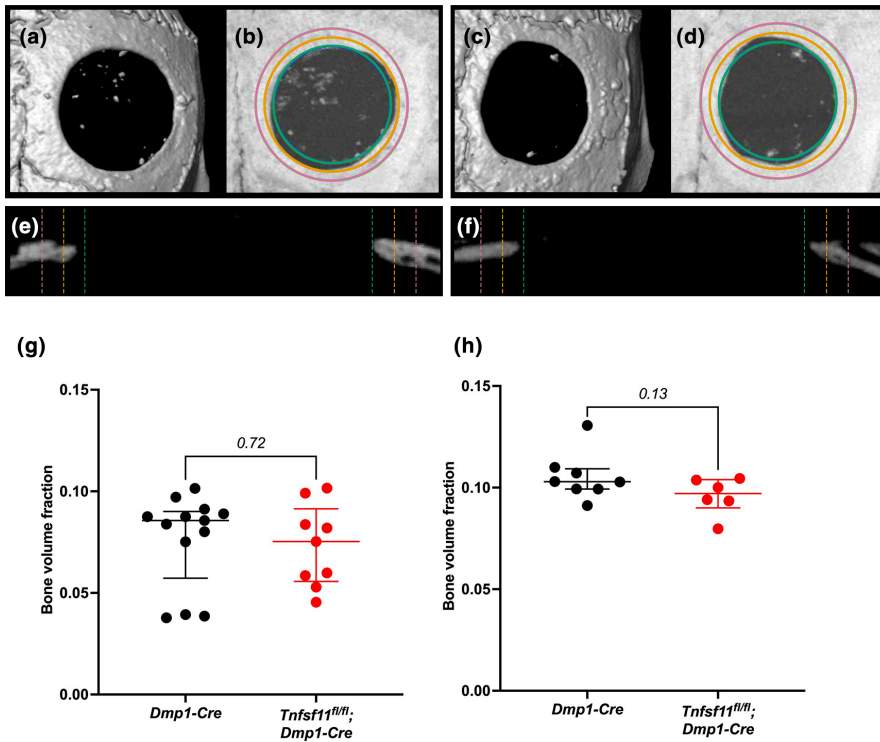


FIGURE 5 Ex vivo micro-computed tomography of the donor area after 4 weeks, showing three-dimensional reconstructions (a, c), maximum intensity projections (b, d) and sagittal views through the defect center (e, f). (a, b, e) *Dmp1-Cre* mouse. (c, d, f) *Tnfsf11^{fl/fl};Dmp1-Cre* mouse. Green, orange, and pink circles and dashed lines represent the defined regions of interest for the micro-computed tomography analyses: circular osteotomy area (green; $d = 3.2$ mm), zone of death (orange; $d_o = 250$ μ m) and safety zone (pink; $d_s = 250$ μ m). (g) Bone volume fraction in the zone of death. (h) Bone volume fraction in the safety zone. Bars and error bars show means and standard deviations, *p*-values using unpaired Student's *t*-tests. All results include data from both male and female mice.

isoenzymes, with some COX-2-selective options available. COX-2 has been shown to play an important role in the bone healing (Simon et al., 2002), and animals lacking it—either through knockout or inhibition (Gerstenfeld & Einhorn, 2004; Zhang et al., 2002)—have shown worse fracture healing. Importantly, this study did not assess the role of COX in bone graft remodeling. In addition, a clinical scenario in which COX inhibitors are administered at such a dosage to influence bone graft consolidation is unlikely. Nonetheless, findings on the link between a transient inflammatory reaction and bone healing are somewhat similar to our findings from subperiosteal grafts in which allowing osteocytes to express RANKL and thereby initiate bone resorption ultimately led to new bone formation.

The limitations of this study can be divided into limitations stemming from the transgenic animal model, the surgeries, and the analyses. One of the main limitations is the off-target activity of the *Dmp1-Cre* model as *Dmp1* is also expressed in mature osteoblasts (Lim et al., 2017; O'Brien et al., 2008) and odontoblasts (Lu et al., 2007). Nonetheless, as dental tissue was not assessed in this study and osteocytic RANKL expression far outweighs that of osteoblasts, we believe that the effects of this off-target activity did not skew our results. Compared with *Dmp1-Cre*, a novel, inducible model driven by the *Sost* promoter has been reported to show lower off-target activity. However, this model is not yet readily obtainable (Maurel et al., 2019). Another important limitation with regard to the surgeries was that for subcutaneous graft placement, a second skin incision was made, resulting in a slight asymmetry among the groups. While the reasoning behind this additional incision was to avoid periosteal damage at the graft site, it might also have been possible to create an aperture in the subcutaneous tissue from the harvesting site and avoid the second skin

incision altogether. With regard to the analyses, this study was limited by its single follow-up point as well as the fact that we did not perform tartrate-resistant acid phosphatase (TRAP) staining to specifically identify osteoclasts in the histological images. This is due to the fact that TRAP staining is not feasible with our light-cured resin embedding system. Consequently, we refrain from explicitly calling the cells of Figure 1d,f osteoclasts.

Within their limitations, our findings can also serve as a primer for future studies by having raised a couple of new questions. First, our data suggest that graft resorption and new bone formation are potentially coupled, an observation that is not surprising per se (Andersen et al., 2013), yet somewhat unexpected when studying autografts. From this, a new hypothesis can be derived, namely that a certain extent of osteoclastic activity is required to initiate the anabolic osteoblast-mediated part of graft consolidation. In this context, our results should be considered preliminary. Testing this new hypothesis will require a more comprehensive study taking these current observations into account. Further, future research could assess to which extent, and if at all, osteocyte-derived RANKL is necessary in various other scenarios of bone regeneration (e.g., socket healing following tooth extraction). Finally, studying graft remodeling following cross-transplantation between *Tnfsf11^{fl/fl};Dmp1-Cre* and *Dmp1-Cre* could help distinguish the role of osteocyte-derived RANKL in the graft and the host.

An auxiliary finding of our study is that the calvarial donor sites of *Tnfsf11^{fl/fl};Dmp1-Cre* and *Dmp1-Cre* mice do not regenerate. This, too, is in agreement with previous work on critical-sized calvarial defects ranging from 1.8 to 2.5 mm in diameter (Cooper et al., 2010; Cowan et al., 2004; Samsonraj et al., 2017). In our defects 3.2 mm in diameter, bone regeneration was limited to the defect borders

(Figure 5). Consequently, we remain unable to draw conclusions on how and whether osteocyte-derived RANKL affects intramembranous bone regeneration. Even though this finding is not related to our original hypothesis, we are reporting it as an additional point of reference for future research using critical-sized calvarial defects. For further investigations, we propose covering the defect with an osteoconductive membrane to serve as a scaffold, which is what we have previously used for calvarial defects in the rat (Feher et al., 2021).

5 | CONCLUSIONS

In the absence of osteocyte-derived RANKL, subcutaneous bone grafts showed virtually no resorption whereas subperiosteal bone grafts showed neither resorption nor new bone formation. Within the limitations of our study, the results suggest an active function of osteocyte-derived RANKL within the bone graft remodeling cascade, identifying osteocyte-derived RANKL as an important factor in the clinical procedure of bone grafting.

AUTHOR CONTRIBUTIONS

BF, JAH, and RG designed the study. BF, CK, and UK performed the surgeries. BF, CK, PH, ST, and RG performed the analyses. BF, CK, and RG interpreted the data. BF and RG wrote the manuscript. JAH and UK critically reviewed the manuscript. All authors have given final approval of the version to be published.

ACKNOWLEDGMENTS

The project was supported by a grant (19–158) from the Osteology Foundation, Switzerland, and a grant (1456/2019) from the ITI Foundation, Switzerland.

CONFLICT OF INTEREST STATEMENT

The authors have no conflicts of interest, financial or otherwise, to disclose.

DATA AVAILABILITY STATEMENT

The data that support the findings of this study are available from the corresponding author upon reasonable request.

ETHICS STATEMENT

All experimental protocols were approved by the Medical University of Vienna institutional animal care and use committee as well as the Austrian Federal Ministry of Education, Science, and Research (No. 2020-0.225.666).

ORCID

Balazs Feher  <https://orcid.org/0000-0003-4386-6237>

Stefan Tangl  <https://orcid.org/0000-0002-9023-4745>

Jill A. Helms  <https://orcid.org/0000-0002-0463-396X>

Ulrike Kuchler  <https://orcid.org/0000-0001-9744-9856>

Reinhard Gruber  <https://orcid.org/0000-0001-5400-9009>

REFERENCES

- Andersen, T. L., Abdelgawad, M. E., Kristensen, H. B., Hauge, E. M., Rolighed, L., Bollerslev, J., Kjærsgaard-Andersen, P., & Delaisse, J. M. (2013). Understanding coupling between bone resorption and formation: Are reversal cells the missing link? *The American Journal of Pathology*, 183(1), 235–246. <https://doi.org/10.1016/j.ajpath.2013.03.006>
- Andreev, D., Liu, M., Weidner, D., Kachler, K., Faas, M., Grüneboom, A., Schlötzer-Schrehardt, U., Muñoz, L. E., Steffen, U., Grötsch, B., Killy, B., Krönke, G., Luebke, A. M., Niemeier, A., Wehrhan, F., Lang, R., Schett, G., & Bozec, A. (2020). Osteocyte necrosis triggers osteoclast-mediated bone loss through macrophage-inducible C-type lectin. *The Journal of Clinical Investigation*, 130(9), 4811–4830. <https://doi.org/10.1172/jci134214>
- Bauer, T. W., & Muschler, G. F. (2000). Bone graft materials. An overview of the basic science. *Clinical Orthopaedics and Related Research*, 371, 10–27.
- Chen, J., Yuan, X., Li, Z., Bahat, D. J., & Helms, J. A. (2020). Bioactivating a bone substitute accelerates graft incorporation in a murine model of vertical ridge augmentation. *Dental Materials*, 36(10), 1303–1313. <https://doi.org/10.1016/j.dental.2020.06.003>
- Chen, X., Wang, H., Wang, Y., Shi, Y., & Wang, Z. (2023). Enhanced osteogenesis by addition of cancellous bone chips at xenogenic bone augmentation: In vitro and in vivo experiments. *Clinical Oral Implants Research*, 34(1), 42–55. <https://doi.org/10.1111/clr.14017>
- Chicana, B., Abbasizadeh, N., Burns, C., Tagliano, H., Spencer, J. A., & Manilay, J. O. (2022). Deletion of Vhl in Dmp1-expressing cells causes microenvironmental impairment of B cell lymphopoiesis. *Frontiers in Immunology*, 13, 780945. <https://doi.org/10.3389/fimmu.2022.780945>
- Cooper, G. M., Mooney, M. P., Gosain, A. K., Campbell, P. G., Losee, J. E., & Huard, J. (2010). Testing the critical size in calvarial bone defects: Revisiting the concept of a critical-size defect. *Plastic and Reconstructive Surgery*, 125(6), 1685–1692. <https://doi.org/10.1097/PRS.0b013e3181cb63a3>
- Cowan, C. M., Shi, Y. Y., Aalami, O. O., Chou, Y. F., Mari, C., Thomas, R., Quarto, N., Contag, C. H., Wu, B., & Longaker, M. T. (2004). Adipose-derived adult stromal cells heal critical-size mouse calvarial defects. *Nature Biotechnology*, 22(5), 560–567. <https://doi.org/10.1038/nbt958>
- Delaisse, J. M. (2014). The reversal phase of the bone-remodeling cycle: Cellular prerequisites for coupling resorption and formation. *BoneKey Reports*, 3, 561. <https://doi.org/10.1038/bonekey.2014.56>
- Dimitriou, R., Jones, E., McGonagle, D., & Giannoudis, P. V. (2011). Bone regeneration: Current concepts and future directions. *BMC Medicine*, 9, 66. <https://doi.org/10.1186/1741-7015-9-66>
- Ding, P., Gao, C., Gao, Y., Liu, D., Li, H., Xu, J., Chen, X., Huang, Y., Zhang, C., Zheng, M., & Gao, J. (2022). Osteocytes regulate senescence of bone and bone marrow. *eLife*, 11. <https://doi.org/10.7554/eLife.81480>
- Feher, B., Apaza Alccayhuaman, K. A., Strauss, F. J., Lee, J. S., Tangl, S., Kuchler, U., & Gruber, R. (2021). Osteoconductive properties of upside-down bilayer collagen membranes in rat calvarial defects. *International Journal of Implant Dentistry*, 7(1), 50. <https://doi.org/10.1186/s40729-021-00333-y>
- Feher, B., Frommlet, F., Ulm, C., Gruber, R., & Kuchler, U. (2022). Preoperative buccal bone volume predicts long-term graft retention following augmentation in the esthetic zone: A retrospective case series. *Clinical Oral Implants Research*, 33(5), 492–500. <https://doi.org/10.1111/clr.13909>
- Fen, J. Q., Zhang, J., Dallas, S. L., Lu, Y., Chen, S., Tan, X., Owen, M., Harris, S. E., & MacDougall, M. (2002). Dentin matrix protein 1, a target molecule for Cbfa1 in bone, is a unique bone marker gene.

- Journal of Bone and Mineral Research*, 17(10), 1822–1831. <https://doi.org/10.1359/jbmr.2002.17.10.1822>
- Fujiwara, Y., Piemontese, M., Liu, Y., Thostenson, J. D., Xiong, J., & O'Brien, C. A. (2016). RANKL (receptor activator of NFκB ligand) produced by osteocytes is required for the increase in B cells and bone loss caused by estrogen deficiency in mice. *The Journal of Biological Chemistry*, 291(48), 24838–24850. <https://doi.org/10.1074/jbc.M116.742452>
- George, A., Sabsay, B., Simonian, P. A., & Veis, A. (1993). Characterization of a novel dentin matrix acidic phosphoprotein. Implications for induction of biomineralization. *The Journal of Biological Chemistry*, 268(17), 12624–12630.
- Gerstenfeld, L. C., & Einhorn, T. A. (2004). COX inhibitors and their effects on bone healing. *Expert Opinion on Drug Safety*, 3(2), 131–136. <https://doi.org/10.1517/eods.3.2.131.27335>
- Graves, D. T., Alshabab, A., Albiero, M. L., Mattos, M., Corrêa, J. D., Chen, S., & Yang, Y. (2018). Osteocytes play an important role in experimental periodontitis in healthy and diabetic mice through expression of RANKL. *Journal of Clinical Periodontology*, 45(3), 285–292. <https://doi.org/10.1111/jcpe.12851>
- Hattner, R., Epker, B. N., & Frost, H. M. (1965). Suggested sequential mode of control of changes in cell behaviour in adult bone remodeling. *Nature*, 206(983), 489–490.
- Hjørting-Hansen, E. (2002). Bone grafting to the jaws with special reference to reconstructive preprosthetic surgery. A historical review. *Mund-, Kiefer- und Gesichtschirurgie*, 6(1), 6–14. <https://doi.org/10.1007/s10006-001-0343-6>
- Huang, E. E., Zhang, N., Ganio, E. A., Shen, H., Li, X., Ueno, M., Utsunomiya, T., Maruyama, M., Gao, Q., Su, N., Yao, Z., Yang, F., Gaudillière, B., & Goodman, S. B. (2022). Differential dynamics of bone graft transplantation and mesenchymal stem cell therapy during bone defect healing in a murine critical size defect. *Journal of Orthopaedic Translation*, 36, 64–74. <https://doi.org/10.1016/j.jot.2022.05.010>
- Insogna, K. L., Sahni, M., Grey, A. B., Tanaka, S., Horne, W. C., Neff, L., Mitnick, M., Levy, J. B., & Baron, R. (1997). Colony-stimulating factor-1 induces cytoskeletal reorganization and c-src-dependent tyrosine phosphorylation of selected cellular proteins in rodent osteoclasts. *The Journal of Clinical Investigation*, 100(10), 2476–2485. <https://doi.org/10.1172/jci119790>
- Kilkenny, C., Browne, W. J., Cuthill, I. C., Emerson, M., & Altman, D. G. (2010). Improving bioscience research reporting: The ARRIVE guidelines for reporting animal research. *PLoS Biology*, 8(6), e1000412. <https://doi.org/10.1371/journal.pbio.1000412>
- Kim, H., Kim, M., Im, S.-K., & Fang, S. (2018). Mouse Cre-LoxP system: General principles to determine tissue-specific roles of target genes. *Laboratory Animal Research*, 34(4), 147–159. <https://doi.org/10.5625/lar.2018.34.4.147>
- Komori, T. (2014). Mouse models for the evaluation of osteocyte functions. *Journal of Bone Metabolism*, 21(1), 55–60. <https://doi.org/10.11005/jbm.2014.21.1.55>
- Kong, Y. Y., Yoshida, H., Sarosi, I., Tan, H. L., Timms, E., Capparelli, C., Morony, S., Oliveira-dos-Santos, A., van, G., Itie, A., Khoo, W., Wakeham, A., Dunstan, C. R., Lacey, D. L., Mak, T. W., Boyle, W. J., & Penninger, J. M. (1999). OPG is a key regulator of osteoclastogenesis, lymphocyte development and lymph-node organogenesis. *Nature*, 397(6717), 315–323. <https://doi.org/10.1038/16852>
- Lee, T.-Y., Lee, K.-I., Dhong, E.-S., Jeong, S.-H., Kim, D.-W., & Han, S.-K. (2022). Long-term resorption rate of autogenous Onlay graft in east Asian rhinoplasty: A retrospective study. *Plastic and Reconstructive Surgery*, 149(2), 360–371. <https://doi.org/10.1097/prs.00000000000008793>
- Leucht, P., Jiang, J., Cheng, D., Liu, B., Dhamdhere, G., Fang, M. Y., Monica, S. D., Urena, J. J., Cole, W., Smith, L. R., Castillo, A. B., Longaker, M. T., & Helms, J. A. (2013). Wnt3a reestablishes osteogenic capacity to bone grafts from aged animals. *The Journal of Bone and Joint Surgery. American Volume*, 95(14), 1278–1288. <https://doi.org/10.2106/jbjs.L.01502>
- Lim, J., Burclaff, J., He, G., Mills, J. C., & Long, F. (2017). Unintended targeting of Dmp1-Cre reveals a critical role for Bmpr1a signaling in the gastrointestinal mesenchyme of adult mice. *Bone Research*, 5, 16049. <https://doi.org/10.1038/boneres.2016.49>
- Lim, K. E., Bullock, W. A., Horan, D. J., Williams, B. O., Warman, M. L., & Robling, A. G. (2021). Co-deletion of Lrp5 and Lrp6 in the skeleton severely diminishes bone gain from sclerostin antibody administration. *Bone*, 143, 115708. <https://doi.org/10.1016/j.bone.2020.115708>
- Lu, Y., Xie, Y., Zhang, S., Dusevich, V., Bonewald, L. F., & Feng, J. Q. (2007). DMP1-targeted Cre expression in odontoblasts and osteocytes. *Journal of Dental Research*, 86(4), 320–325. <https://doi.org/10.1177/154405910708600404>
- Maiorana, C., Beretta, M., Salina, S., & Santoro, F. (2005). Reduction of autogenous bone graft resorption by means of bio-Oss coverage: A prospective study. *The International Journal of Periodontics & Restorative Dentistry*, 25(1), 19–25.
- Maurel, D. B., Matsumoto, T., Vallejo, J. A., Johnson, M. L., Dallas, S. L., Kitase, Y., Brotto, M., Wacker, M. J., Harris, M. A., Harris, S. E., & Bonewald, L. F. (2019). Characterization of a novel murine Sost ER. *Bone Research*, 7, 6. <https://doi.org/10.1038/s41413-018-0037-4>
- McCutcheon, S., Majeska, R. J., Spray, D. C., Schaffler, M. B., & Vazquez, M. (2020). Apoptotic osteocytes induce RANKL production in bystanders via purinergic signaling and activation of pannexin channels. *Journal of Bone and Mineral Research*, 35(5), 966–977. <https://doi.org/10.1002/jbmr.3954>
- Mendes, B. C., Pereira, R. D. S., Mourão, C., Montemezzi, P., Santos, A. M. S., Moreno, J. M. L., Okamoto, R., & Hochuli-Vieira, E. (2022). Evaluation of two Beta-tricalcium phosphates with different particle dimensions in human maxillary sinus floor elevation: A prospective, randomized clinical trial. *Materials (Basel)*, 15(5). <https://doi.org/10.3390/ma15051824>
- Meza-Mauricio, J., Furquim, C. P., dos Reis, L., Maximiano, M. M., Mendoza-Azpur, G., Muniz, F. W., Rasperini, G., & Faveri, M. (2022). How efficacious is the combination of substitute bone graft with autogenous bone graft in comparison with substitute bone graft alone in the horizontal bone gain? A systematic review and meta-analysis. *Journal of Clinical and Experimental Dentistry*, 14(8), e678–e688. <https://doi.org/10.4317/jced.59087>
- Nakashima, T., Hayashi, M., Fukunaga, T., Kurata, K., Oh-Hora, M., Feng, J. Q., Bonewald, L. F., Kodama, T., Wutz, A., Wagner, E. F., Penninger, J. M., & Takayanagi, H. (2011). Evidence for osteocyte regulation of bone homeostasis through RANKL expression. *Nature Medicine*, 17(10), 1231–1234. <https://doi.org/10.1038/nm.2452>
- O'Brien, C. A., Plotkin, L. I., Galli, C., Goellner, J. J., Gortazar, A. R., Allen, M. R., Robling, A. G., Bouxsein, M., Schipani, E., Turner, C. H., Jilka, R. L., Weinstein, R. S., Manolagas, S. C., & Bellido, T. (2008). Control of bone mass and remodeling by PTH receptor signaling in osteocytes. *PLoS One*, 3(8), e2942. <https://doi.org/10.1371/journal.pone.0002942>
- Ono, T., Hayashi, M., Sasaki, F., & Nakashima, T. (2020). RANKL biology: Bone metabolism, the immune system, and beyond. *Inflammation and Regeneration*, 40, 2. <https://doi.org/10.1186/s41232-019-01111-3>
- Park, J. H., Lee, N. K., & Lee, S. Y. (2017). Current understanding of RANK signaling in osteoclast differentiation and maturation. *Molecules and Cells*, 40(10), 706–713. <https://doi.org/10.14348/molcells.2017.0225>
- Sakkas, A., Wilde, F., Heufelder, M., Winter, K., & Schramm, A. (2017). Autogenous bone grafts in oral implantology—is it still a "gold standard"? A consecutive review of 279 patients with 456 clinical procedures. *International Journal of Implant Dentistry*, 3(1), 23. <https://doi.org/10.1186/s40729-017-0084-4>
- Salem, D., Natto, Z., Elangovan, S., & Karimbux, N. (2016). Usage of bone replacement grafts in periodontics and Oral implantology and their

- current levels of clinical evidence — A systematic assessment. *Journal of Periodontology*, 87(8), 872–879. <https://doi.org/10.1902/jop.2016.150512>
- Samsornraj, R. M., Dudakovic, A., Zan, P., Pichurin, O., Cool, S. M., & van Wijnen, A. J. (2017). A versatile protocol for studying Calvarial bone defect healing in a mouse model. *Tissue Engineering. Part C, Methods*, 23(11), 686–693. <https://doi.org/10.1089/ten.TEC.2017.0205>
- Sbordone, C., Toti, P., Guidetti, F., Califano, L., Santoro, A., & Sbordone, L. (2012). Volume changes of iliac crest autogenous bone grafts after vertical and horizontal alveolar ridge augmentation of atrophic maxillas and mandibles: A 6-year computerized tomographic follow-up. *Journal of Oral and Maxillofacial Surgery*, 70(11), 2559–2565. <https://doi.org/10.1016/j.joms.2012.07.040>
- Shoji-Matsunaga, A., Ono, T., Hayashi, M., Takayanagi, H., Moriyama, K., & Nakashima, T. (2017). Osteocyte regulation of orthodontic force-mediated tooth movement via RANKL expression. *Scientific Reports*, 7(1), 8753. <https://doi.org/10.1038/s41598-017-09326-7>
- Simon, A. M., Manigrasso, M. B., & O'Connor, J. P. (2002). Cyclooxygenase 2 function is essential for bone fracture healing. *Journal of Bone and Mineral Research*, 17(6), 963–976. <https://doi.org/10.1359/jbmr.2002.17.6.963>
- Stevenson, S., Li, X. Q., & Martin, B. (1991). The fate of cancellous and cortical bone after transplantation of fresh and frozen tissue-antigen-matched and mismatched osteochondral allografts in dogs. *The Journal of Bone and Joint Surgery. American Volume*, 73(8), 1143–1156.
- Stricker, A., Jacobs, R., Maes, F., Fluegge, T., Vach, K., & Fleiner, J. (2021). Resorption of retromolar bone grafts after alveolar ridge augmentation-volumetric changes after 12 months assessed by CBCT analysis. *International Journal of Implant Dentistry*, 7(1), 7. <https://doi.org/10.1186/s40729-020-00285-9>
- Toyosawa, S., Shintani, S., Fujiwara, T., Oshima, T., Sato, A., Ijuhin, N., & Komori, T. (2001). Dentin matrix protein 1 is predominantly expressed in chicken and rat osteocytes but not in osteoblasts. *Journal of Bone and Mineral Research*, 16(11), 2017–2026. <https://doi.org/10.1359/jbmr.2001.16.11.2017>
- Troeltzsch, M., Troeltzsch, M., Kauffmann, P., Gruber, R., Brockmeyer, P., Moser, N., Rau, A., & Schliephake, H. (2016). Clinical efficacy of grafting materials in alveolar ridge augmentation: A systematic review. *Journal of Cranio-Maxillo-Facial Surgery*, 44(10), 1618–1629. <https://doi.org/10.1016/j.jcms.2016.07.028>
- Wang, L., Aghvami, M., Brunski, J., & Helms, J. (2017). Biophysical regulation of osteotomy healing: An animal study. *Clinical Implant Dentistry and Related Research*, 19(4), 590–599. <https://doi.org/10.1111/cid.12499>
- Xiong, J., & O'Brien, C. A. (2012). Osteocyte RANKL: New insights into the control of bone remodeling. *Journal of Bone and Mineral Research*, 27(3), 499–505. <https://doi.org/10.1002/jbmr.1547>
- Xiong, J., Onal, M., Jilka, R. L., Weinstein, R. S., Manolagas, S. C., & O'Brien, C. A. (2011). Matrix-embedded cells control osteoclast formation. *Nature Medicine*, 17(10), 1235–1241. <https://doi.org/10.1038/nm.2448>
- Xiong, J., Piemontese, M., Onal, M., Campbell, J., Goellner, J. J., Dusevich, V., Bonewald, L., Manolagas, S. C., & O'Brien, C. A. (2015). Osteocytes, not osteoblasts or lining cells, are the Main source of the RANKL required for osteoclast formation in remodeling bone. *PLoS One*, 10(9), e0138189. <https://doi.org/10.1371/journal.pone.0138189>
- Xiong, J., Piemontese, M., Thostenson, J. D., Weinstein, R. S., Manolagas, S. C., & O'Brien, C. A. (2014). Osteocyte-derived RANKL is a critical mediator of the increased bone resorption caused by dietary calcium deficiency. *Bone*, 66, 146–154. <https://doi.org/10.1016/j.bone.2014.06.006>
- Zhang, X., Schwarz, E. M., Young, D. A., Puzas, J. E., Rosier, R. N., & O'Keefe, R. J. (2002). Cyclooxygenase-2 regulates mesenchymal cell differentiation into the osteoblast lineage and is critically involved in bone repair. *The Journal of Clinical Investigation*, 109(11), 1405–1415. <https://doi.org/10.1172/jci15681>
- Zhang, X., Xie, C., Lin, A. S., Ito, H., Awad, H., Lieberman, J. R., Rubery, P. T., Schwarz, E. M., O'Keefe, R. J., & Goldberg, R. E. (2005). Periosteal progenitor cell fate in segmental cortical bone graft transplantations: Implications for functional tissue engineering. *Journal of Bone and Mineral Research*, 20(12), 2124–2137. <https://doi.org/10.1359/jbmr.050806>
- Zhao, R., Yang, R., Cooper, P. R., Khurshid, Z., Shavandi, A., & Ratnayake, J. (2021). Bone grafts and substitutes in dentistry: A review of current trends and developments. *Molecules*, 26(10). <https://doi.org/10.3390/molecules26103007>

SUPPORTING INFORMATION

Additional supporting information can be found online in the Supporting Information section at the end of this article.

How to cite this article: Feher, B., Kamleitner, C., Heimel, P., Tangl, S., Helms, J. A., Kuchler, U., & Gruber, R. (2023). The effect of osteocyte-derived RANKL on bone graft remodeling: An in vivo experimental study. *Clinical Oral Implants Research*, 00, 1–11. <https://doi.org/10.1111/clr.14187>